Molecular Pharmacology Fast Forward. Published on May 8, 2009 as doi:10.1124/mol.109.055756

Functional importance of a structurally-distinct homo-dimeric complex of the Family B G protein-coupled secretin receptor

Fan Gao, Kaleeckal G. Harikumar, Maoqing Dong, Polo C.-H. Lam, Patrick M. Sexton, Arthur Christopoulos, Andrew Bordner, Ruben Abagyan, Laurence J. Miller

F.G., K.G.H., M.D., A.B., L.J.M., Department of Molecular Pharmacology and Experimental Therapeutics, Mayo Clinic, Scottsdale, AZ 85259;

P.C.-H.L, R.A., Scripps Research Institute, Department of Molecular Biology and Molsoft, LLC, La Jolla, CA 92037;

P.M.S., A.C, Drug Discovery Biology Laboratory, Monash Institute of Pharmaceutical Sciences and Department of Pharmacology, Monash University, Melbourne 3800, Australia

Molecular Pharmacology Fast Forward. Published on May 8, 2009 as DOI: 10.1124/mol.109.055756
This article has not been copyedited and formatted. The final version may differ from this version.

Running title: Dimeric secretin receptor

Non-standard abbreviations: BRET, bioluminescence resonance energy transfer; COS, African green monkey kidney; cuprous phenanthroline (CuP); DSS, disuccinimidyl suberate; GPCR, G protein-coupled receptor; GppNHp, 5'-guanylimidodiphosphate; ICM, internal coordinate mechanics; KRH, Kreb's-Ringer-HEPES; Rlu, *Renilla* luciferase; TM, transmembrane segment; YFP, yellow fluorescence protein.

Address correspondence to:

Laurence J. Miller, M.D.
Mayo Clinic
13400 East Shea Boulevard
Scottsdale, AZ 85259
Telephone: (480)-301-6650
Fax: (480)-301-6969
E-mail: miller@mayo.edu

Number of text pages: 35
Number of tables: 4
Number of figures: 9
Number of references: 44
Number of words in Abstract: 258
Number of words in Introduction: 594
Number of words in Discussion: 1167

Molecular Pharmacology Fast Forward. Published on May 8, 2009 as DOI: 10.1124/mol.109.055756
This article has not been copyedited and formatted. The final version may differ from this version.

ABSTRACT

Oligomerization of G protein-coupled receptors has been described, but its structural basis and functional importance have been inconsistent. Here, we demonstrate that the agonist occupied wild type secretin receptor is predominantly in a guanine nucleotide sensitive high affinity state and exhibits negative cooperativity, while the monomeric receptor is primarily in a guanine nucleotide insensitive lower affinity state. We previously demonstrated constitutive homo-dimerization of this receptor through the lipid-exposed face of TM IV. We now use cysteine-scanning mutagenesis of fourteen TM IV residues, bioluminescence resonance energy transfer (BRET), and functional analysis to map spatial approximations and functional importance of specific residues in this complex. All, except for three helix-facing mutants, trafficked to the cell surface, where secretin was shown to bind and elicit cAMP production. Cells expressing complementary-tagged receptors were treated with cuprous phenanthroline to establish disulfide bonds between spatially-approximated cysteines. BRET was measured as an indication of receptor oligomerization, and was repeated after competitive disruption of oligomers with TM IV peptide to distinguish covalent from non-covalent associations. While all constructs generated a significant BRET signal, this was disrupted by peptide in all except for single site mutants replacing five residues with cysteine. Of these, covalent stabilization of receptor homo-dimers through positions of Gly^{243}, Ile^{247}, and Ala^{250} resulted in a GTP-sensitive high affinity state of the receptor, while the same procedure with Ala^{246} and Phe^{240} mutants resulted in a GTP-insensitive lower affinity state. We propose the existence of a functionally-important, structurally-specific high affinity dimeric state of the secretin receptor, which may be typical of Family B G protein-coupled receptors.

Molecular Pharmacology Fast Forward. Published on May 8, 2009 as DOI: 10.1124/mol.109.055756
This article has not been copyedited and formatted. The final version may differ from this version.

Dimerization of single transmembrane tyrosine kinase receptors is well recognized as a critically important mechanism for the complementary cross-phosphorylation and activation of these receptors (Overton et al., 2003). Oligomerization has also been reported for heptahelical guanine nucleotide-binding protein (G protein)-coupled receptors (GPCRs) (Milligan, 2008), but the structural rules and functional implications of these interactions are not well understood. Some receptors are thought to self-associate (homo-oligomerization) while some can associate with other receptors (hetero-oligomerization); both of these events are described as occurring constitutively or in response to agonist occupation, or even with such occupation disrupting oligomeric complexes (Ayoub et al., 2004; Carrillo et al., 2003; Cheng and Miller, 2001; Ding et al., 2002). There are reports of the state of GPCR oligomerization affecting affinity of natural ligands, changing the selectivity of ligand binding, modifying biological responses, and affecting receptor regulation (Albizu et al., 2006; Franco et al., 2008; Hague et al., 2006; Milligan and Smith, 2007; Stanasila et al., 2003) . No clear rules yet exist for the specificity of receptor association or for its functional implications. There is even less understood regarding the valency of the oligomeric complexes, and how structurally distinct these complexes may be.

We previously demonstrated constitutive, agonist-independent homo-oligomerization of the Family B secretin receptor (Ding et al., 2002). Of particular interest, this was also demonstrated to reflect the dimeric state, rather than a higher-order oligomeric state (Harikumar et al., 2008a) . Consistent with that interpretation, there was no effect of the extracellular amino-terminal tail region or the intracellular carboxyl-terminal tail region on dimerization, with only one of seven transmembrane (TM) segments, the fourth such segment (TM IV), contributing to the interaction

Molecular Pharmacology Fast Forward. Published on May 8, 2009 as DOI: 10.1124/mol.109.055756
This article has not been copyedited and formatted. The final version may differ from this version.

(Harikumar et al., 2007). That report identified the lipid-exposed residues, Gly^{243} and Ile^{247}, as playing a key role in the dimerization (Harikumar et al., 2007).

The goal of the current project was to extend our understanding of the homo-dimeric state of the secretin receptor, both structurally and functionally. We used cysteine-scanning mutagenesis of fourteen residues within TM IV. All constructs were fully characterized to ensure normal biosynthesis, trafficking, and surface expression, as well as their functional integrity. Receptor constructs tagged at the carboxyl terminus with *Renilla* luciferase (Rlu) or with yellow fluorescence protein (YFP) were studied using bioluminescence resonance energy transfer (BRET) before and after treatment with cuprous phenanthroline (CuP), an oxidizing reagent that promotes the formation of disulfide bonds between spatially-approximated cysteine residues. BRET was measured as an indication of oligomerization, and was repeated after specific competitive disruption of oligomers with synthetic secretin receptor TM IV peptide to distinguish covalent from non-covalent associations between the receptor constructs. Radioligand binding was performed to assess the functional status of the particular complexes. Of particular interest, only a subset of the lipid-facing residues within TM IV were found to be capable of forming disulfide-bonded homo-dimeric complexes reflecting their symmetrical spatial approximation, and only a further subset of these were able to establish the normal high affinity state of this receptor reflecting structural specificity of this important functional state of the receptor.

The combination of the observations of homo-dimerization of the secretin receptor without higher-order oligomerization (Harikumar et al., 2008a), a structurally-specific single interface for the

Molecular Pharmacology Fast Forward. Published on May 8, 2009 as DOI: 10.1124/mol.109.055756
This article has not been copyedited and formatted. The final version may differ from this version.

dimers (Harikumar et al., 2007), and differential functional impact of different dimeric receptor structures, provides strong evidence for the existence of a functionally-important, structurally-specific high affinity homo-dimeric state of this receptor. This theme may also be typical of Family B G protein-coupled receptors, with the association of multiple members of this family with the secretin receptor already demonstrated (Harikumar et al., 2006b; Harikumar et al., 2008b).

Molecular Pharmacology Fast Forward. Published on May 8, 2009 as DOI: 10.1124/mol.109.055756
This article has not been copyedited and formatted. The final version may differ from this version.

Materials and Methods

Materials. Reagents for molecular biological techniques were obtained from New England Biolabs (Beverly, MA), Stratagene (La Jolla, CA), Eppendorf (Hamburg, Germany), and Qiagen (Valencia, CA). A 27-amino acid peptide representing secretin receptor transmembrane segment IV (TM IV) was synthesized as described previously (Harikumar et al., 2007). Coelenterazine *h* was from Biotium (Hayward, CA). The [Tyr^{10}]secretin peptide was radioiodinated with the solid-phase oxidant, iodobeads (Pierce Chemical Co., Rockford, IL), and purified using reversed-phase HPLC to yield a specific radioactivity of approximately 2000 Ci/mmol.

Plasmids and mutagenesis. Recombinant human secretin receptor constructs tagged with Rlu or YFP in frame at its carboxyl terminus were subcloned into the eukaryotic expression vector, pcDNA3.0 (Invitrogen), as described previously (Harikumar et al., 2007). Receptor point mutations were prepared using the QuikChange^{TM} kit from Stratagene (La Jolla, CA). Each of the mutated receptor constructs was confirmed by direct DNA sequence analysis.

Cell cultures and transfection. African green monkey kidney (COS) cells were used for the transient expression of receptor constructs. These were grown in Dulbecco's Modified Eagle's Medium (DMEM) supplemented with Fetal Clone II (Hyclone, Logan, UT) on tissue culture plasticware in a humidified atmosphere of 5% CO_2 at 37 ^{o}C. The cells were transfected with the wild type and mutant secretin receptor constructs using diethylaminoethyl-dextran (DEAE-dextran) solutions, as described previously (Harikumar et al., 2006b). For each 10 cm Petri dish, 3 μg of plasmid DNA was typically added (unless noted otherwise). For co-expression of Rlu- and YFP-tagged constructs, 1.5 μg of each

Molecular Pharmacology Fast Forward. Published on May 8, 2009 as DOI: 10.1124/mol.109.055756
This article has not been copyedited and formatted. The final version may differ from this version.

plasmid DNA was added. Cells or their receptor-bearing membranes were studied 48 to 72 h after transfection to allow maximal levels of expression of recombinant protein. Particulate preparations enriched in plasma membranes bearing the secretin receptors were prepared using the sucrose density gradient centrifugation method previously described (Hadac et al., 1996).

Fluorescence microscopy. Biosynthesis and cellular trafficking of receptor constructs were evaluated by visualizing fluorescence in COS cells expressing YFP-tagged receptor constructs. The transfected cells grown on 25 mm coverslips were fixed and mounted on microscopic slides. YFP fluorescence was acquired using appropriate spectral settings (excitation, 488 nm argon laser; emission, LP505 filter; pinhole diameter 2.3 airy units) of the Zeiss LSM 510 confocal microscope (Thornwood, NY) equipped with a Plan-Apochromat 63X/1.4 numerical aperture oil objective.

Characterization of secretin receptor binding. To characterize the ability of receptor constructs to bind secretin, transfected intact cells grown in 24-well plates were studied using a radioligand binding assay. Cells were first washed twice with Kreb's-Ringer-HEPES (KRH) medium (25 mM HEPES, pH 7.4, 104 mM NaCl, 5 mM KCl, 1 mM KH_2PO_4, 2 mM $CaCl_2$, and 1.2 mM $MgSO_4$) supplemented with 0.2% bovine serum albumin and 0.01% soybean trypsin inhibitor . The cells were then incubated with a constant amount of the cell-impermeant radioligand, [^{125}I-Tyr^{10}]secretin (approximately 30,000 dpm), and increasing concentrations of unlabeled secretin (from 0 to 1 μM) for 1 h at room temperature to achieve binding equilibrium. Cell-bound radioactivity was quantified with a γ-spectrometer. Non-saturable binding was determined in the presence of 1 μM unlabeled secretin and represented less than 20% of total binding.

Molecular Pharmacology Fast Forward. Published on May 8, 2009 as DOI: 10.1124/mol.109.055756
This article has not been copyedited and formatted. The final version may differ from this version.

More detailed analysis of secretin binding was performed using plasma membranes expressing wild type and mutant receptors in analogous assays. Rapid separation of bound from free radioligand was performed by centrifugation at 14,000 rpm at 4 ^{o}C, and washing twice with ice-cold KRH medium. All assays were performed in duplicate in a minimum of three independent experiments. Data were graphed using the Prism program (GraphPad Software, San Diego, CA) and were analyzed using LIGAND (Munson and Rodbard, 1980).

Binding cooperativity was evaluated in a radioligand binding dissociation assay, comparing dissociation of receptor-bound radioligand in the presence of "infinite dilution" (achieved by washing cells and resuspending them in ligand-free buffer) with that in the presence of "infinite dilution" plus a saturating concentration of secretin. Secretin radioligand dissociation was studied in membranes from receptor-bearing cells after allowing receptors to be occupied with [^{125}I-Tyr^{10}]secretin after incubation at 4 ^{o}C for 60 min. At that time, cells were washed and resuspended in KRH medium at room temperature in the absence or presence of 1 μM secretin. Bound and free radioligand were quantified at various points in time up to 40 min.

Characterization of cAMP responses of secretin receptors. To characterize the ability of receptor constructs stimulated with secretin to produce cAMP, transfected intact cells grown in 96-well plates had their cAMP responses to secretin analyzed. Briefly, cells were washed with phosphate-buffered saline (PBS) (154 mM NaCl, 8.1 mM Na_2HPO_4, and 1.9 mM NaH_2PO_4, pH 7.4) and were exposed to increasing amounts of secretin (from 0 to 1 μM) diluted in KRH medium supplemented with 0.2%

Molecular Pharmacology Fast Forward. Published on May 8, 2009 as DOI: 10.1124/mol.109.055756
This article has not been copyedited and formatted. The final version may differ from this version.

bovine serum albumin, 0.01% soybean trypsin inhibitor, 0.1% bacitracin and 1 mM 3-isobutyl-1-methylxanthine for 30 min at 37 ^{o}C. The cells then were lysed using acid and neutralized, as described previously (Harikumar et al., 2007). The resulting supernatants were utilized in a fluorescence-based competitive-binding cAMP assay (PerkinElmer, Wellesley, MA) that utilizes a Europium tag and Alexa Fluor® 647 in a 384-well white Optiplate, with LANCE kit and the 2103 Envision plate reader. Detection was based on time-resolved fluorescence resonance energy transfer.

Receptor cross-linking. Chemical cross-linking of wild type and mutant secretin receptors was performed in PBS. Transfected intact COS cells or enriched receptor-bearing membranes prepared from transfected COS cells were treated with thiol-reactive cross-linker, cuprous phenanthroline (final concentration 1 mM), or with the amine-reactive bifunctional chemical cross-linker, disuccinimidyl suberate (final concentration 50 μM), for 10 min. Reactions were terminated by addition of EDTA (final concentration 20 mM) or Tris·HCl, pH 7.4 (final concentration 50 mM), respectively, followed by washing with KRH medium, in preparation for the subsequent BRET and receptor-binding studies.

Bioluminescence resonance energy transfer (BRET) assays. Bioluminescence and fluorescence measurements were performed with aliquots of approximately 25,000 transfected intact COS cells co-expressing receptors tagged with Rlu and YFP, as described previously (Harikumar et al., 2007). 48 h after transfection, the cells were lifted with non-enzymatic dissociation solution, and were resuspended in PBS solution. The cells treated with or without cross-linking reagents were incubated with synthetic secretin receptor TM IV peptide (40 μg/ml) for 2 h before performing the BRET assay. For comparison, the BRET signals from the cells without the competitive incubation with receptor

Molecular Pharmacology Fast Forward. Published on May 8, 2009 as DOI: 10.1124/mol.109.055756
This article has not been copyedited and formatted. The final version may differ from this version.

TM IV peptide were also measured to reflect receptor oligomerization (independent of the establishment of covalent stabilization). The BRET assay was initiated by adding the cell-permeant *Renilla* luciferase-specific substrate, coelenterazine *h*, to the cell suspension to yield a final concentration of 5 μM in a 96-well white Optiplate (Perkin-Elmer, Wellesley, MA). Bioluminescence (from Rlu) and fluorescence (from YFP) intensities at 475 nm and 525 nm respectively were read in the 2103 Envision fluorescence plate reader (Perkin-Elmer, Wellesley, MA). The BRET ratios were calculated based on the ratios of emission (Harikumar et al., 2007).

BRET titration (saturation) experiments were performed to validate the observations in the static BRET studies (Harikumar et al., 2007). For this, COS cells were transfected both with a constant amount of donor construct (Rlu-tagged receptor construct at a concentration of 1.0 μg DNA/0.5 x 10^6 cells) and with increasing amounts of acceptor construct (YFP-tagged receptor construct at concentrations of 0.3 to 6.0 μg DNA/0.5 x 10^6 cells). BRET assays were performed 48 h after transfection with or without treatment with cuprous phenanthroline, as described above.

Statistical analysis. Statistical analysis was performed with the GraphPad Prism software version 4.0 (La Jolla, CA), using the unpaired t-test. Differences with $P<0.05$ were considered to be statistically significant.

Molecular modeling. All molecular modeling activities for this project were implemented in the Internal Coordinate Mechanics (ICM) program (Abagyan, 1994). This procedure consisted of three iterative steps: (a) random conformational change of a dihedral angle according to the

Molecular Pharmacology Fast Forward. Published on May 8, 2009 as DOI: 10.1124/mol.109.055756
This article has not been copyedited and formatted. The final version may differ from this version.

biased-probability Monte Carlo method (Abagyan and Totrov, 1994); (b) local minimization of all free dihedral angles; and (c) acceptance or rejection of the new conformation based on the Metropolis criterion at the simulation temperature, usually around 600 K (Metropolis N, 1953). This approach can generate and search through diverse sets of molecular conformations by actively sampling a selected set of dihedral angles.

The peptide representing TM IV of the secretin receptor was initially studied in isolation to examine possible modes of peptide dimerization. All-atom models of interacting TM IV segments were created using molecular mechanics simulations combined with distance restraints derived from experimental cross-linking results. Restraints were included for both cross-linking of residues that promoted secretin receptor dimerization in the high-affinity state (Gly^{243}, Ile^{247}, and Ala^{250}) and those that did not lead to covalently associated dimerization (Gln^{235}, Gly^{236}, Ala^{239}, Ser^{244}, Phe^{248}, and Val^{249}). Separations between C_β (C_α for glycine) atoms for cross-linked residue pairs were restrained to be in the range of 3.2 – 8.0 Å (2.2 – 5.5 Å for glycine). These distance ranges were determined by increasing the typical separation range of these atoms in disulfide bonds by a 1.5 Å margin in order to allow for limited structural flexibility. Separations between the corresponding atoms of non-cross-linked residues were constrained to be larger than the upper limit of these distance ranges.

Because proline residues often induce bends in transmembrane helices (Reiersen and Rees, 2001), two sets of simulations with different protein backbone geometry were performed, one with ideal alpha helix angles (ϕ = -60°, ψ = -45°) and another with a large angle bend at Pro^{245}. The backbone torsion angles for the bend were taken from a transmembrane segment in an X-ray structure that has a

Molecular Pharmacology Fast Forward. Published on May 8, 2009 as DOI: 10.1124/mol.109.055756
This article has not been copyedited and formatted. The final version may differ from this version.

relatively large 37° proline-induced bend (residues 72-95 from PDB: 2RH1). The molecular mechanics simulations were started from 300 different initial conformations and sampled the relative orientations of the helices as well as side chain torsion angles. The simulations were performed using the ICM program (Molsoft LLC, version 3.5) which performed Monte Carlo global optimization of an energy function that included van der Waals, hydrogen bond, electrostatic, and torsion terms from the ECEPP/3 force field (Nemethy et al., 1992) as well as an area-based entropic term. All simulations were run for 5×10^6 Monte Carlo steps at a temperature of 500 K.

Molecular models of the intact secretin receptor (Dong et al., 2008) homo-dimeric complex were also generated. For this, the Arg^{231} to Arg^{255} segment of the secretin receptor representing TM IV was constructed in ICM, including the sampling and minimization of all side chain and backbone variables. A copy of this helical segment was generated; all the side chain, backbone, and five of the six positional variables of the two copies of TM IV were linked to impose a two-fold symmetry throughout subsequent modeling. Distance restraints with an upper limit of 6.5 Å were imposed between the C_α of Gly^{243}, Ile^{247}, and Ala^{250} of the two TM IV units. All the positional and side chain variables were sampled in six independent runs until they converged to a single solution. The backbone variables were further minimized. This procedure has been tested on the dimerization interface of Anabaena sensory rhodopsin (PDB: 1XIO, final model 0.6 Å C_α rmsd from experimental structure) and Gcn-4 leucine zipper (PDB: 1ZIK, final model 0.8 Å C_α rmsd from experimental structure).

To build a model of the transmembrane helical bundle domain of the secretin receptor, the

Molecular Pharmacology Fast Forward. Published on May 8, 2009 as DOI: 10.1124/mol.109.055756
This article has not been copyedited and formatted. The final version may differ from this version.

"cold-spot" method was utilized with the crystal structure of the human β2-adrenergic receptor as template (Cherezov et al., 2007). The recently reported TM bundle and loop modeling method was used (Dong et al., 2008). The backbone variables of TM IV were fixed during the whole procedure to maintain the integrity of the dimerization interface. After simulation, a full atomic model of the transmembrane domain was constructed by connecting the helical bundle with the loops in one continuous chain. The 100 best energy conformations were retained. For each of these conformations, a second copy of the full TM helical bundle region was generated and the dimerization interface was constructed between the two TM IV segments. All the side chains involved in the dimerization interface were minimized in the preparation of the final intact receptor homo-dimer model.

Results

The sequence and proposed orientation of TM IV of the secretin receptor relative to the adjacent transmembrane helices and the lipid bilayer are shown in Figure 1. This orientation was based on the sequence analysis of Family B G protein-coupled receptors by Donnelly (Donnelly, 1997), as well as sequence alignment and homology modeling with the crystal structures of rhodopsin and the β2-adrenergic receptor based on the cold-spot method (Frimurer and Bywater, 1999). Both methods provided similar proposed topology and orientation of secretin receptor TM IV.

All of the cysteine-replacement secretin receptor mutants were tagged with either Rlu or YFP to enable tracking of receptor distribution and for study of receptor dimerization by BRET. Of note, both Rlu- and YFP-tagged receptors have been reported to behave similarly to wild type secretin receptor

Molecular Pharmacology Fast Forward. Published on May 8, 2009 as DOI: 10.1124/mol.109.055756
This article has not been copyedited and formatted. The final version may differ from this version.

(Harikumar et al., 2007). All but three of the fourteen mutants trafficked to the cell surface (Fig. 2). The three constructs that did not reach the cell surface (G241C, W242C, and P245C secretin receptor mutants) involved mutations of residues predicted to face another transmembrane helical segment and likely resulted in aberrant helical packing and aggregation. Consistent with this, none of these three constructs displayed any recognizable secretin binding or secretin-stimulated biological activity in the intact cells (Table 1). Intact COS cells transiently expressing each of the other cysteine-replacement mutants displayed saturable binding of cell-impermeant secretin peptide with affinities close to that of wild type secretin receptor, and secretin-stimulated biological activity with potencies also similar to that of wild type secretin receptor (Table 1).

We have previously established the homo-dimeric nature of the secretin receptor using a broad variety of techniques, including BRET and morphological FRET (Lisenbee and Miller, 2006). We also applied a transmembrane segment peptide-competition assay to establish that only TM IV contributed to the dimeric receptor interface, and we reported that the simultaneous replacement of two lipid-facing residues with alanines (Gly^{243} and Ile^{247}) could disrupt the complex (Harikumar et al., 2007). Here, we have taken a systematic analysis of residues within TM IV, individually studying eleven residues within TM IV (excluding the three residues where cysteine-replacement mutants were not active) to carefully map the dimeric interface. Of note, in addition to BRET, we have now added the approach of scanning cysteine-replacement mutagenesis with covalent stabilization using cuprous phenanthroline, and we have attempted to disrupt the complexes in a structurally-specific manner using the natural TM IV peptide as an indication of the covalent nature of the disulfide bonding between the constructs. Positive controls for dimeric receptor constructs were complexes stabilized

Molecular Pharmacology Fast Forward. Published on May 8, 2009 as DOI: 10.1124/mol.109.055756
This article has not been copyedited and formatted. The final version may differ from this version.

covalently by the bifunctional amine-reactive crosslinker, disuccinimidyl suberate (DSS).

The results of application of this assay are illustrated in Figure 3. In this assay, we only observed positive receptor BRET signals with receptor constructs capable of forming dimers, with the G243A/I247A double mutant exhibiting no significant BRET signal. Each of the receptor cysteine mutant constructs that trafficked to the cell surface was capable of forming a homo-dimeric complex, as reflected by a positive BRET signal above background. This signal was stabilized covalently using DSS, resulting in a receptor dimer that was not disrupted by competition with the TM IV peptide, in all of these constructs. In the absence of cross-linker, TM IV competition always significantly reduced these BRET signals to near background levels.

The cuprous phenanthroline treatment identified a subset of cysteine-replacement mutants that had their cysteine residues in adequate spatial approximation and appropriate geometry to form covalent symmetrical homo-dimers bound by disulfide bonds (Fig 3). These comprised those constructs with cysteines in positions 240, 243, 246, 247, and 250 that were resistant to dissociation with the TM IV peptide. It is noteworthy that mutants with cysteines in positions 239, 244, 248, and 249, immediately adjacent to residues at which disulfide bonds were established, were not covalently stabilized with the cuprous phenanthroline. It is also quite interesting that mutants with cysteine replacing lipid-facing residues in positions 235 and 236 also failed to form disulfide bonds. These are one helix turn before residue 240, which is one of the sites of successful disulfide formation. Another key control is also shown in Figure 3, representing the assay of cells co-expressing Rlu-tagged G243C mutant and YFP-tagged I247C mutant, both of which are capable of forming

Molecular Pharmacology Fast Forward. Published on May 8, 2009 as DOI: 10.1124/mol.109.055756
This article has not been copyedited and formatted. The final version may differ from this version.

disulfide-bonded symmetrical homo-dimers. Under these assay conditions, it was clear that the constructs formed hetero-dimeric receptor complexes, but there were no disulfide bonds between these two receptor constructs in these complexes. This provided further evidence of the structural specificity of the assay, without effect of cysteine oxidation independent of disulfide formation.

An additional important control was added, representing BRET titration studies to further validate the static BRET results. These have been utilized to distinguish a significant, saturable BRET signal from a bystander effect that could result from random interactions of donor and acceptor (Harikumar et al., 2007) . Shown in Figure 4 is a typical assay applied to one construct representing a cuprous phenanthroline-stabilized receptor dimer (I247C) and one construct representing a homo-dimer not stabilized by cuprous phenanthroline (A239C). In this assay, both constructs yielded typical two-phase saturation BRET curves that increased rapidly before reaching an asymptote. For both constructs, this was reduced to a single-phase curve not statistically different from a straight line when the incubation was performed in the presence of TM IV peptide. The cuprous phenanthroline incubations clearly distinguished the differential behavior of the two constructs. The presence of this reagent did not modify the saturation BRET signal for either construct, but the addition of TM IV peptide disrupted the saturation BRET signal from the A239C construct, but not the I247C construct. This provides evidence that only the I247C secretin receptor construct was covalently stabilized by a cuprous phenanthroline-induced disulfide bond, with such a bond absent from the homo-dimeric A239C receptor construct.

The secretin receptor is a typical G protein-coupled receptor, with its G protein-coupled state

Molecular Pharmacology Fast Forward. Published on May 8, 2009 as DOI: 10.1124/mol.109.055756
This article has not been copyedited and formatted. The final version may differ from this version.

recognized as the high affinity state of the receptor (Harikumar et al., 2006a). Indeed, the secretin competition-binding curve for the wild type secretin receptor was shallow, reflecting both high affinity and low affinity binding sites (Fig 5). As shown in this figure, the non-hydrolyzable analogue of GTP, 5'-guanylimidodiphosphate (GppNHp), moved the wild type secretin receptor binding curve to the right, significantly shifting the high affinity state toward lower affinity. The quantitative analysis of these binding curves is shown in Table 2.

It is particularly interesting to compare the secretin competition-binding data for the mutant secretin receptor that does not form dimers (G243A/I247A) to that observed with wild type secretin receptor (Fig 5 and Table 2). The non-dimerizing double mutant exhibited lower affinity binding than that observed for the wild type receptor, with the competition-binding curve not significantly affected by GppNHp. This is consistent with less efficient G protein coupling for the non-dimerizing construct. It is thus possible that the homo-dimeric receptor construct facilitates G protein coupling.

The other interesting feature of the dimeric, but not the monomeric, form of the secretin receptor was the clear evidence for negative binding cooperativity. The classical approach for detecting negative cooperativity is to monitor the dissociation of labeled secretin in the absence or presence of unlabeled secretin using an “infinite dilution” procedure. At the wild-type (dimeric) receptor, radiolabeled secretin exhibited essentially monophasic dissociation over the time-course of the assay with a dissociation rate constant (K) of 0.33±0.13 min^{-1} ($t_{1/2}$ =2.09 min), although the beginning of an undefined slow phase of dissociation could be discerned. However, in the presence of secretin, a clear biphasic dissociation was observed with a poorly defined rapid phase ($t_{1/2}$~0.19 min; K_2=3.54±4.65

Molecular Pharmacology Fast Forward. Published on May 8, 2009 as DOI: 10.1124/mol.109.055756
This article has not been copyedited and formatted. The final version may differ from this version.

min^{-1}) and a distinct slower phase with a dissociation rate of 0.14±0.02 ($t_{1/2}$=4.86 min) (Fig 6, upper panel). In contrast, at the non-dimerizing G243A/I247A form of the receptor, dissociation of radiolabeled secretin was not altered in the presence of the unlabeled peptide; both exhibiting essentially monophasic dissociation, with dissociation constants of 0.06±0.02 min^{-1} and 0.07±0.02 min^{-1} in the absence and presence of unlabelled secretin, respectively (Fig 6, lower panel).

The cross-linking studies (Fig 3) identified five residues of the lipid face of TM IV that supported dimer formation. These residues are located throughout the transmembrane domain with up to 60 degrees difference in predicted rotational position. Such differences would likely yield markedly distinct conformations, only some of which would be expected to support efficient G protein interaction. We, therefore, studied the effect of cuprous phenanthroline on the binding profile of each of the secretin receptor cysteine-replacement mutants that were able to form disulfide-bonded receptor dimers (Fig 7). Like wild type secretin receptor, each of these constructs exhibited shallow competition-binding curves, reflective of both high and low affinity states (Table 3). Of note, two patterns can be readily seen for the effect of the treatment on these constructs. In one pattern, the treatment kept the receptor binding characteristics similar to the wild type receptor (G243C, I247C, and A250C). In the other pattern, the treatment resulted in a significant reduction in the affinity value for the high affinity state (F240C and A246C) (Table 3). Exemplars of each of these two phenotypes (G243C and A246C, respectively) were subsequently evaluated for GTP-dependency of the binding of cuprous phenanthroline-treated constructs. As shown in Figure 8, the G243C mutant remained sensitive to GppNHp, leading to a marked decrease in affinity in the presence of this nucleotide. In contrast, the A246C mutant remained in a lower affinity conformation that was

Molecular Pharmacology Fast Forward. Published on May 8, 2009 as DOI: 10.1124/mol.109.055756
This article has not been copyedited and formatted. The final version may differ from this version.

insensitive to GppNHp.

To provide a structural context for our experimental data molecular models of the secretin receptor dimer interface were generated. Modeling the structures of the isolated peptide dimeric helical structures was performed first. The TM IV segments were modeled both as ideal α-helices and with Pro^{245}-induced bends in their centers. The lowest energy conformations of the TM IV helix dimer for both of these conformations included a left-handed crossing angle. In fact, all conformations having energies within 5 kcal/mol of the lowest attained energy for this structure had left-handed crossing angles. The separation of the alpha helix axes was 9.3 Å for the straight helices and 8.4 Å for the bent helices. The predicted crossing angles are within the distribution observed for parallel left-handed helix pairs and the separation distances are typical for membrane proteins (Walters and DeGrado, 2006). The concordance between the results for these two extremes of helix bending angles, namely no bend and a bend angle near the maximum observed in known membrane protein structures, suggests that TM IV helices adopt a left-handed crossing angle, independent of the helix bending angle.

Shown in Figure 9 is a representation of the best three-dimensional molecular model of the intact secretin receptor homo-dimeric complex. In the final model, the crossing angle between two neighboring TM IV segments is 30º, similar to that observed in the dimerization interface of Anabaena sensory rhodopsin and Gcn-4 leucine zipper. Table 4 lists the C_β to C_β distances between the residues along this segment that were studied in this work. It is noteworthy that those residues that were capable of forming disulfide bonds when replaced by cysteines were within 9.2 Å of each other in the

Molecular Pharmacology Fast Forward. Published on May 8, 2009 as DOI: 10.1124/mol.109.055756
This article has not been copyedited and formatted. The final version may differ from this version.

intact homo-dimeric receptor model, while those that did not form such bonds were generally greater than 12 Å, with a few exceptions where distance may have been adequate, but geometry was not. It is also important that the predicted secretin-binding pocket in the receptor extracellular amino-terminal tail domain resides at the opposite sides of the dimeric interface, likely providing adequate room for each receptor protomer to bind one secretin peptide ligand. The G protein-binding site has not yet been mapped sufficiently for a Family B GPCR to reliably place it in this model. The proximity of Pro^{245} to the helical interface would allow it to form a flexible hinge that may contribute to conformational transitions across dimers, as has been seen in other membrane proteins (Sansom and Weinstein, 2000; Yohannan et al., 2004)

Molecular Pharmacology Fast Forward. Published on May 8, 2009 as DOI: 10.1124/mol.109.055756
This article has not been copyedited and formatted. The final version may differ from this version.

Discussion

While GPCR oligomerization has been reported to exist for more than ten years (Hebert JBC 1996), much remains to be understood about its structure and function. There may well be distinct themes for the different families of GPCRs. The best current understanding of this phenomenon exists for Family C GPCRs, where crystal structures for covalently bonded amino-terminal domains have been solved (Kunishima et al., 2000; White et al., 1998). Hetero-dimerization of some Family C GPCRs has been shown to be critical for cell surface expression and for receptor function (Ciruela et al., 2001; Ferre et al., 2002). The largest number of reports for GPCR oligomerization occur for Family A receptors (Park et al., 2004) . Here, however, there has been substantial variation in structural and functional themes reported (Hernanz-Falcon et al., 2004; Park et al., 2004; Salahpour et al., 2004). Despite clear evidence for the ability of some of these GPCRs to associate, there are also clear recent evidence for receptors in this family (the β2-adrenergic receptor (Whorton et al., 2007) and rhodopsin (Whorton et al., 2008)) to be fully functional in their monomeric states, where kinetics of agonist binding and G protein coupling are entirely normal. Analogous studies have not yet been reported for a Family B GPCR.

Indeed, evidence is mounting that structurally-specific homo-dimerization may be an important structural theme that has critical functional implications for Family B GPCRs. This is clearly true for the prototypic secretin receptor. In recent reports, this receptor has been shown to exhibit constitutive oligomerization that is not disrupted by agonist stimulation (Harikumar et al., 2006b). Systematic investigation of the portion of the secretin receptor that contributes to the oligomerization eliminated the amino-terminal tail and carboxyl-terminal tail regions, and established that only TM IV

Molecular Pharmacology Fast Forward. Published on May 8, 2009 as DOI: 10.1124/mol.109.055756
This article has not been copyedited and formatted. The final version may differ from this version.

of the seven transmembrane segments contributed significantly to this (Harikumar et al., 2007). Further, only the lipid-exposed face of TM IV was found to be important, and two residues within that face, Gly^{243} and Ile^{247} were identified as contributing (Harikumar et al., 2007). In the current report, this initial observation has been substantially extended with the systematic evaluation of 14 residues within this segment, and with the careful functional characterization of disulfide-linked cysteine replacement mutants in spatial approximation with each other. This has demonstrated key functional differences for specific structural complexes.

It is noteworthy that most of the cysteine-replacement secretin receptor mutants underwent normal biosynthesis and trafficking to the cell surface, where they were shown to be fully functional. Only mutations of three helix-facing residues, Gly^{241}, Trp^{242}, and Pro^{245}, interfered with normal cell surface expression. All other mutants, including those tagged at the carboxyl terminus with *Renilla* luciferase or with yellow fluorescent protein, trafficked to the cell surface, where the cell-impermeant natural peptide ligand, secretin, was shown to bind normally and to elicit normal cAMP signals. Cells expressing the complementary-tagged receptors were treated with cuprous phenanthroline, an oxidizing reagent that promotes the formation of disulfide bonds between spatially-approximated cysteine residues. BRET was measured as an indication of oligomerization, and was repeated after competitive disruption of oligomers with synthetic TM IV peptide to distinguish covalent from non-covalent associations between donor- and acceptor-tagged receptor constructs.

Non-disruptable BRET signals were observed for the cuprous phenanthroline-treated secretin receptor mutants in which residues Phe^{240}, Gly^{243}, Ala^{246}, Ile^{247}, and Ala^{250} were replaced with cysteine,

Molecular Pharmacology Fast Forward. Published on May 8, 2009 as DOI: 10.1124/mol.109.055756
This article has not been copyedited and formatted. The final version may differ from this version.

supporting the ability to form covalent symmetrical dimers for these constructs. In contrast, cysteines in positions of residues Ala^{239}, Ser^{244}, Phe^{248}, and Val^{249}, as well as two lipid-facing residues low in the helix (Gln^{235} and Gly^{236}), had BRET signals disrupted by the peptide, suggesting distance and/or geometry of the cysteines that were incompatible with disulfide bond formation. Careful radioligand binding analysis revealed that secretin bound to two affinity states of this receptor, with the wild type receptor predominantly exhibiting its G protein-coupled high affinity state, and with the monomeric receptor mutant residing predominantly in a G protein-uncoupled lower affinity state. Further, only the homo-dimeric state of the secretin receptor exhibited negative binding cooperativity. Of particular note, receptor dimers covalently stabilized through the positions of Gly^{243}, Ile^{247}, or Ala^{250} retained the prerequisite flexibility that is required for efficient conformational transition and efficient G protein-coupling, while the same procedure with the Phe^{240} and Ala^{246} mutants stabilized the receptor into a GTP-insensitive, lower affinity state.

The three-dimensional molecular modeling of the homo-dimeric secretin receptors provided additional insights into potential behavior of the dimeric receptor complex. The isolated TM IV helix models established that imposition of a severe proline-induced kink in the helix, something that has not been experimentally established or refuted, had very little impact on the geometry of the dimerization interface, with all low energy models simultaneously satisfying both positive and negative experimentally-derived distance restraints. The alignment of these helices was also quite similar to that in the intact homo-dimeric secretin receptor model.

It is also of interest that the predicted secretin peptide-binding pocket within the receptor amino

Molecular Pharmacology Fast Forward. Published on May 8, 2009 as DOI: 10.1124/mol.109.055756
This article has not been copyedited and formatted. The final version may differ from this version.

terminus is at the opposite side of the receptor to the dimeric interface. This suggests that a secretin peptide should be able to bind to each of the receptor protomers in the dimeric complex, yielding a 1:1 stoichiometry. There is substantial opportunity for the amino-terminal domains of the receptor protomers to interact with each other, possibly affecting their conformations. This could contribute to the substantial negative cooperativity of secretin ligand binding observed in the dimeric wild type receptor that was not observed for the non-dimerizing dual mutant secretin receptor. Additional experimental constraints will be necessary to model the amino-terminal domains in the intact dimeric receptors in a meaningful way.

Heterotrimeric G proteins are known to interact with the cytosolic face of GPCRs, with many examples of the importance of the third intracellular loop region and portions of the second intracellular loop and carboxyl-terminal tail (Claus et al., 2006; Kostenis et al., 1997). The most extensive analysis of this interaction involves Family A GPCRs (Heydorn et al., 2004; Kostenis et al., 1997). Much less is currently known about the G protein-binding site within Family B GPCRs. With the current observation that the non-dimerizing secretin receptor dual mutant had its secretin binding much less affected by GppNHp, a non-hydrolyzable analogue of GTP, than that of wild type secretin receptor, it is likely that the dimeric structure facilitates G protein binding and this is consistent with the large decrease in agonist potency observed for the non-dimerising receptor mutant, in cAMP accumulation studies (Harikumar et al., 2007). The structural basis of this are not yet clear.

This work has provided important new insights into the structure of the homo-dimeric secretin receptor. The structural specificity of the fully active dimer is highlighted by the two distinct

Molecular Pharmacology Fast Forward. Published on May 8, 2009 as DOI: 10.1124/mol.109.055756
This article has not been copyedited and formatted. The final version may differ from this version.

phenotypes exhibited by individual disulfide-bonded cysteine-replacement mutants, while structural modeling of the receptor-receptor interaction provides a potential mechanistic framework for conformational transition across the dimer. Further studies are required to understand the implications of this structure for G protein binding to the cytosolic face of the complex, and whether these themes are consistent for other members of this physiologically-important receptor family.

Molecular Pharmacology Fast Forward. Published on May 8, 2009 as DOI: 10.1124/mol.109.055756
This article has not been copyedited and formatted. The final version may differ from this version.

Acknowledgments

The authors thank R. Happs, A.S. Ball, and M.L. Augustine for their excellent technical assistance.

Molecular Pharmacology Fast Forward. Published on May 8, 2009 as DOI: 10.1124/mol.109.055756
This article has not been copyedited and formatted. The final version may differ from this version.

References

Abagyan R and Totrov M (1994) Biased probability Monte Carlo conformational searches and electrostatic calculations for peptides and proteins. *J Mol Biol* **235**:983-1002.

Abagyan RA, Totrov, M.M., and Kuznetsov, D.A. (1994) Icm: A New Method For Protein Modeling and Design: Applications To Docking and Structure Prediction From The Distorted Native Conformation. *J Comp Chem* **15**:488-506.

Albizu L, Balestre MN, Breton C, Pin JP, Manning M, Mouillac B, Barberis C and Durroux T (2006) Probing the existence of G protein-coupled receptor dimers by positive and negative ligand-dependent cooperative binding. *Mol Pharmacol* **70**:1783-1791.

Ayoub MA, Levoye A, Delagrange P and Jockers R (2004) Preferential formation of MT1/MT2 melatonin receptor heterodimers with distinct ligand interaction properties compared with MT2 homodimers. *Mol Pharmacol* **66**:312-321.

Carrillo JJ, Pediani J and Milligan G (2003) Dimers of class A G protein-coupled receptors function via agonist-mediated trans-activation of associated G proteins. *J Biol Chem* **278**:42578-42587.

Cheng ZJ and Miller LJ (2001) Agonist-dependent dissociation of oligomeric complexes of G protein-coupled cholecystokinin receptors demonstrated in living cells using bioluminescence resonance energy transfer. *J Biol Chem* **276**:48040-48047.

Cherezov V, Rosenbaum DM, Hanson MA, Rasmussen SG, Thian FS, Kobilka TS, Choi HJ, Kuhn P, Weis WI, Kobilka BK and Stevens RC (2007) High-resolution crystal structure of an engineered human beta2-adrenergic G protein-coupled receptor. *Science* **318**:1258-1265.

Ciruela F, Escriche M, Burgueno J, Angulo E, Casado V, Soloviev MM, Canela EI, Mallol J, Chan WY, Lluis C, McIlhinney RA and Franco R (2001) Metabotropic glutamate 1alpha and adenosine A1 receptors assemble into functionally interacting complexes. *J Biol Chem* **276**:18345-18351.

Claus M, Neumann S, Kleinau G, Krause G and Paschke R (2006) Structural determinants for G-protein activation and specificity in the third intracellular loop of the thyroid-stimulating hormone receptor. *J Mol Med* **84**:943-954.

Ding WQ, Cheng ZJ, McElhiney J, Kuntz SM and Miller LJ (2002) Silencing of secretin receptor function by dimerization with a misspliced variant secretin receptor in ductal pancreatic adenocarcinoma. *Cancer Res* **62**:5223-5229.

Dong M, Lam PC, Pinon DI, Sexton PM, Abagyan R and Miller LJ (2008) Spatial approximation between secretin residue five and the third extracellular loop of its receptor provides new insight into the molecular basis of natural agonist binding. *Mol Pharmacol* **74**:413-422.

Dong M, Wang Y, Hadac EM, Pinon DI, Holicky E and Miller LJ (1999) Identification of an interaction between residue 6 of the natural peptide ligand and a distinct residue within the amino-terminal tail of the secretin receptor. *J Biol Chem* **274**:19161-19167.

Donnelly D (1997) The arrangement of the transmembrane helices in the secretin receptor family of G-protein-coupled receptors. *FEBS Lett* **409**:431-436.

Ferre S, Karcz-Kubicha M, Hope BT, Popoli P, Burgueno J, Gutierrez MA, Casado V, Fuxe K, Goldberg SR, Lluis C, Franco R and Ciruela F (2002) Synergistic interaction between adenosine A2A and glutamate mGlu5 receptors: implications for striatal neuronal function. *Proc Natl Acad Sci U S A* **99**:11940-11945.

Franco R, Casado V, Cortes A, Mallol J, Ciruela F, Ferre S, Lluis C and Canela EI (2008) G-protein-coupled receptor heteromers: function and ligand pharmacology. *Br J Pharmacol* **153 Suppl 1**:S90-98.

Frimurer TM and Bywater RP (1999) Structure of the integral membrane domain of the GLP1 receptor. *Proteins* **35**:375-386.

Hadac EM, Ghanekar DV, Holicky EL, Pinon DI, Dougherty RW and Miller LJ (1996) Relationship between native and recombinant cholecystokinin receptors: role of differential glycosylation. *Pancreas* **13**:130-139.

Hague C, Lee SE, Chen Z, Prinster SC, Hall RA and Minneman KP (2006) Heterodimers of alpha1B- and alpha1D-adrenergic receptors form a single functional entity. *Mol Pharmacol* **69**:45-55.

Harikumar KG, Happs RM and Miller LJ (2008a) Dimerization in the absence of higher-order oligomerization of the G protein-coupled secretin receptor. *Biochim Biophys Acta* **1778**:2555-2563.

Harikumar KG, Hosohata K, Pinon DI and Miller LJ (2006a) Use of probes with fluorescence indicator distributed throughout the pharmacophore to examine the peptide agonist-binding environment of the family B G protein-coupled secretin receptor. *J Biol Chem* **281**:2543-2550.

Harikumar KG, Morfis MM, Lisenbee CS, Sexton PM and Miller LJ (2006b) Constitutive formation of oligomeric complexes between family B G protein-coupled vasoactive intestinal polypeptide and secretin receptors. *Mol Pharmacol* **69**:363-373.

Harikumar KG, Morfis MM, Sexton PM and Miller LJ (2008b) Pattern of intra-family hetero-oligomerization involving the G-protein-coupled secretin receptor. *J Mol Neurosci* **36**:279-285.

Harikumar KG, Pinon DI and Miller LJ (2007) Transmembrane segment IV contributes a functionally important interface for oligomerization of the Class II G protein-coupled secretin receptor. *J Biol Chem* **282**:30363-30372.

Hernanz-Falcon P, Rodriguez-Frade JM, Serrano A, Juan D, del Sol A, Soriano SF, Roncal F, Gomez L, Valencia A, Martinez AC and Mellado M (2004) Identification of amino acid residues crucial for chemokine receptor dimerization. *Nat Immunol* **5**:216-223.

Heydorn A, Ward RJ, Jorgensen R, Rosenkilde MM, Frimurer TM, Milligan G and Kostenis E (2004) Identification of a novel site within G protein alpha subunits important for specificity of receptor-G protein interaction. *Mol Pharmacol* **66**:250-259.

Kostenis E, Gomeza J, Lerche C and Wess J (1997) Genetic analysis of receptor-Galphaq coupling selectivity. *J Biol Chem* **272**:23675-23681.

Kunishima N, Shimada Y, Tsuji Y, Sato T, Yamamoto M, Kumasaka T, Nakanishi S, Jingami H and Morikawa K (2000) Structural basis of glutamate recognition by a dimeric metabotropic glutamate receptor. *Nature* **407**:971-977.

Lisenbee CS and Miller LJ (2006) Secretin receptor oligomers form intracellularly during maturation through receptor core domains. *Biochemistry* **45**:8216-8226.

Metropolis N RA, Rosenbluth MN, Teller AH and Teller E (1953) Equation of State Calculations by Fast Computing Machines. *J Chem Phys* **21**:1087-1092.

Milligan G (2008) A day in the life of a G protein-coupled receptor: the contribution to function of G protein-coupled receptor dimerization. *Br J Pharmacol* **153 Suppl 1**:S216-229.

Milligan G and Smith NJ (2007) Allosteric modulation of heterodimeric G-protein-coupled receptors.

Trends Pharmacol Sci **28**:615-620.

Munson PJ and Rodbard D (1980) Ligand: a versatile computerized approach for characterization of ligand-binding systems. *Anal Biochem* **107**:220-239.

Nemethy G, Gibson KD, Palmer KA, Yoon CN, Paterlini G, Zagari A, Rumsey S and Scheraga HA (1992) Energy Parameters in Polypeptides. 10. Improved geometric parameters and nonbonded interactions for use in the ECEPP/3 algorithm, with application to proline-containing peptides. *J Phys Chem* **96**:6472-6484.

Overton MC, Chinault SL and Blumer KJ (2003) Oligomerization, biogenesis, and signaling is promoted by a glycophorin A-like dimerization motif in transmembrane domain 1 of a yeast G protein-coupled receptor. *J Biol Chem* **278**:49369-49377.

Park PS, Filipek S, Wells JW and Palczewski K (2004) Oligomerization of G protein-coupled receptors: past, present, and future. *Biochemistry* **43**:15643-15656.

Reiersen H and Rees AR (2001) The hunchback and its neighbours: proline as an environmental modulator. *Trends Biochem Sci* **26**:679-684.

Salahpour A, Angers S, Mercier JF, Lagace M, Marullo S and Bouvier M (2004) Homodimerization of the beta2-adrenergic receptor as a prerequisite for cell surface targeting. *J Biol Chem* **279**:33390-33397.

Sansom MS and Weinstein H (2000) Hinges, swivels and switches: the role of prolines in signalling via transmembrane alpha-helices. *Trends Pharmacol Sci* **21**:445-451.

Stanasila L, Perez JB, Vogel H and Cotecchia S (2003) Oligomerization of the alpha 1a- and alpha 1b-adrenergic receptor subtypes. Potential implications in receptor internalization. *J Biol Chem* **278**:40239-40251.

Walters RF and DeGrado WF (2006) Helix-packing motifs in membrane proteins. *Proc Natl Acad Sci U S A* **103**:13658-13663.

White JH, Wise A, Main MJ, Green A, Fraser NJ, Disney GH, Barnes AA, Emson P, Foord SM and Marshall FH (1998) Heterodimerization is required for the formation of a functional GABA(B) receptor. *Nature* **396**:679-682.

Whorton MR, Bokoch MP, Rasmussen SG, Huang B, Zare RN, Kobilka B and Sunahara RK (2007) A monomeric G protein-coupled receptor isolated in a high-density lipoprotein particle efficiently activates its G protein. *Proc Natl Acad Sci U S A* **104**:7682-7687.

Whorton MR, Jastrzebska B, Park PS, Fotiadis D, Engel A, Palczewski K and Sunahara RK (2008) Efficient coupling of transducin to monomeric rhodopsin in a phospholipid bilayer. *J Biol Chem* **283**:4387-4394.

Yohannan S, Faham S, Yang D, Whitelegge JP and Bowie JU (2004) The evolution of transmembrane helix kinks and the structural diversity of G protein-coupled receptors. *Proc Natl Acad Sci U S A* **101**:959-963.

Molecular Pharmacology Fast Forward. Published on May 8, 2009 as DOI: 10.1124/mol.109.055756
This article has not been copyedited and formatted. The final version may differ from this version.

Footnotes

This work was supported by grants from the National Institutes of Health [DK46577] and the Fiterman Foundation, as well as Mayo Clinic.

Molecular Pharmacology Fast Forward. Published on May 8, 2009 as DOI: 10.1124/mol.109.055756
This article has not been copyedited and formatted. The final version may differ from this version.

Figure legends

Fig. 1. Proposed topology, with depth and orientation of human secretin receptor TM IV residues. Shown is the predicted helical wheel organization of residues within TM III, IV, and V of this receptor (adapted from the GLP-1 receptor model of Donnelly (Donnelly, 1997). Residues displayed with white lettering (in grey and black circles) represent the fourteen residues studied by cysteine-replacement mutagenesis in the current work, with those predicted to be lipid-exposed displayed as black filled circles with white lettering. Residue numbering is based on the sequence of the intact wild type human secretin receptor after cleavage of the leader sequence (Dong et al., 1999).

Fig. 2. Confocal microscopic images of YFP-tagged secretin receptor constructs. Shown are representative examples of COS cells expressing the YFP-tagged wild type secretin receptor and the fourteen TM IV cysteine-replacement mutants. All except for G241C, W242C and P245C mutants show significant YFP fluorescence on the cell surface. All images were acquired under similar settings and were representative of at least three independent experiments.

Fig. 3. Effect of cross-linking on secretin receptor BRET. Shown are BRET ratios for COS cells expressing the wild type (WT) and alanine- or cysteine-replacement mutants of the secretin receptor in the absence or presence of competing TM IV peptide and in the absence or presence of amine-reactive (disuccinimidyl suberate, DSS) or sulfhydryl-reactive (cuprous phenanthroline, CuP) cross-linking. The *shaded area* represents the nonspecific BRET signal that can be generated between Rlu-tagged receptor and soluble YFP protein or between YFP-tagged receptor and soluble Rlu (0.056), with BRET signals above this area considered to be significant. The data are presented as the means ±

S.E.M. of 3-4 independent experiments. The values marked with ** represent BRET signals significantly different from those obtained with same receptor-expressing cells incubated without TM peptide in the absence and presence of cross-linking at the $p<0.001$ level. Highlighted in the frame are the BRET signal differences between dimeric wild type and monomeric G243A/I247A secretin receptor constructs.

Fig. 4. Saturation BRET analysis of receptor cysteine-replacement mutants. Shown are the BRET saturation curves plotted as ratios of YFP fluorescence to Rlu luminescence that were observed for tagged receptor constructs studied with a fixed amount of donor and increasing amounts of acceptor. Both A239C and I247C secretin receptor constructs yielded exponential curves that reached asymptotes indicating significant oligomerization. This was disrupted to yield curves not different from a straight line when the same incubations were performed in the presence of receptor TM IV peptide. The CuP studies yielded saturable BRET signals for both constructs, with the I247C construct signal not disrupted by TM IV peptide, while the A239C construct signal was disrupted, reflecting absence of a covalent disulfide bond.

Fig. 5. The effect of GppNHp on secretin radioligand binding to dimeric and monomeric secretin receptors. Shown are curves for secretin competing for binding of [^{125}I-Tyr^{10}]secretin to membranes from COS cells expressing the dimeric (wild type, WT) and monomeric (G243A/I247A) secretin receptor constructs in the absence and presence of 10 μM GppNHp. Values represent percentages of maximal saturable binding that were observed in the absence of secretin. They are expressed as means ± S.E.M. of duplicate data from three independent experiments.

Molecular Pharmacology Fast Forward. Published on May 8, 2009 as DOI: 10.1124/mol.109.055756
This article has not been copyedited and formatted. The final version may differ from this version.

Fig. 6. Negative cooperativity of secretin binding to the secretin receptor homo-dimer. Shown are secretin radioligand binding dissociation curves over time, induced by "infinite dilution" in the absence and presence of a saturating concentration of secretin, for both wild type receptor and for the non-dimerizing G243A/I247A secretin receptor construct. Secretin induced more rapid dissociation of bound radioligand only at the wild type receptor.

Fig. 7. Characterization of secretin receptor binding in COS cell membranes. Shown are curves for secretin competition for binding of [^{125}I-Tyr^{10}]secretin to membranes from COS cells expressing the wild type (WT) and alanine- or cysteine-replacement mutants in the absence and presence of cuprous phenanthroline. Values represent percentages of maximal saturable binding that were observed in the absence of secretin. They are expressed as means ± S.E.M. of duplicate data from three independent experiments. CuP, cuprous phenanthroline.

Fig. 8. GTP-sensitivity of secretin binding in cuprous phenantroline-stabilized cysteine mutants of the secretin receptor. Shown are secretin competition-binding curves to cuprous phenanthroline (CuP)-treated membranes from COS cells expressing two cysteine-replacement mutants in the absence and presence of GppNHp, a non-hydrolyzable analogue of GTP. Values represent percentages of maximal saturable binding that were observed in the absence of secretin. They are expressed as means ± S.E.M. of duplicate data from three independent experiments.

Fig. 9. Molecular model of the intact secretin receptor homo-dimeric complex. Shown is the best

Molecular Pharmacology Fast Forward. Published on May 8, 2009 as DOI: 10.1124/mol.109.055756
This article has not been copyedited and formatted. The final version may differ from this version.

secretin receptor homo-dimer model. The transmembrane domain is colored blue-red from the amino terminus to the carboxyl terminus. The three residues Gly^{243}, Ile^{247}, and Ala^{250}, were represented by ball-and-stick. *Top*, the dimerization interface between two secretin receptor monomers is shown. *Bottom*, the secretin receptor homo-dimer model is superimposed with the latest secretin-bound receptor model. The secretin peptide is colored blue-red from the amino terminus to the carboxyl terminus. The amino-terminal domain of the receptor is colored purple. Green wire: Phe^{240}, Ala^{246}. Orange wire: Gln^{235}, Gly^{236}, Ala^{239}, Ser^{244}, Phe^{248}, Val^{249}. Red wire: Gly^{241}, Trp^{242}, Pro^{245}.

Molecular Pharmacology Fast Forward. Published on May 8, 2009 as DOI: 10.1124/mol.109.055756
This article has not been copyedited and formatted. The final version may differ from this version.

TABLE 1

Pharmacological characteristics of Rlu-tagged secretin receptor constructs expressed in intact COS cells

Shown are the IC_{50} values of secretin binding to COS cells expressing each of the noted secretin receptor constructs. Shown also are EC_{50} values for secretin-stimulated intracellular cAMP responses in these cells, as well as E_{max} values reflecting maximal cAMP concentrations achieved. Values are expressed as means ± S.E.M. of data from at least three independent experiments. [1]All the YFP-tagged constructs behaved similarly to the complementary Rlu-tagged constructs. [2]ND: Not determined.

Rlu-tagged receptors[1]	IC_{50} (nM)	EC_{50} (nM)	E_{max} (pmol/10^6 cells)
WT	3.9 ± 0.5	0.31 ± 0.05	198 ± 46
Q235C	7.6 ± 0.6	0.51 ±0.11	185 ± 50
G236C	3.3 ± 1.0	0.49 ± 0.10	201 ± 44
A239C	4.9 ± 0.5	0.64 ±0.14	187 ± 49
F240C	3.2 ± 0.6	0.72 ± 0.15	188 ± 38
G241C	Not detected	ND[2]	ND[2]
W242C	Not detected	ND[2]	ND[2]
G243C	5.0 ± 0.6	0.39 ± 0.13	195 ± 43
S244C	4.2 ± 0.9	0.25 ± 0.04	190 ± 33
P245C	Not detected	ND[2]	ND[2]
A246C	4.6 ± 0.1	0.39 ± 0.09	193 ± 35
I247C	5.0 ± 0.6	0.36 ± 0.08	188 ± 40
F248C	3.0 ± 0.3	0.41 ± 0.08	196 ± 46
V249C	4.3 ± 1.1	0.76 ± 0.19	200 ± 52
A250C	5.0 ± 1.6	0.65 ± 0.12	197 ± 47

Molecular Pharmacology Fast Forward. Published on May 8, 2009 as DOI: 10.1124/mol.109.055756
This article has not been copyedited and formatted. The final version may differ from this version.

TABLE 2

Binding parameters of the dimeric wild type and a monomeric mutant form of the secretin receptor in COS cell membranes

[#]high – high affinity site; low – low affinity site. *significantly different from the same receptor construct studied in the absence of GppNHp, $p<0.05$. Values are expressed as means ± S.E.M. of data from three independent experiments.

	pK_i ([#]high)	pK_i ([#]low)	B_{max} ([#]high) *pmol/mg*	B_{max} ([#]low) *pmol/mg*
WT	8.62 ± 0.15	6.52 ± 0.19	7.2 ± 1.5	187 ± 3
WT (GppNHp)	*8.03 ± 0.22	6.48 ± 0.22	9.1 ± 2.3	127 ± 36
G243A/I247A	8.14 ± 0.08	6.55 ± 0.22	9.7 ± 1.5	138 ± 36
G243A/I247A (GppNHp)	7.87 ± 0.07	6.31 ± 0.17	8.5 ± 0.8	152 ± 42

Molecular Pharmacology Fast Forward. Published on May 8, 2009 as DOI: 10.1124/mol.109.055756
This article has not been copyedited and formatted. The final version may differ from this version.

TABLE 3

Binding parameters of cysteine mutants of the secretin receptor in the absence or presence of cuprous phenanthroline (CuP), in comparison with wild type and non-dimerizing double mutant secretin receptor

[#]high – high affinity site; low – low affinity site. [$]significantly different from the wild type receptor, $p<0.05$. *significantly different from the same receptor construct studied in the absence of cuprous phenanthroline, $p<0.05$. Values are expressed as means ± S.E.M. of data from three independent experiments.

	pK_i ([#]high)	pK_i ([#]low)	B_{max} ([#]high) *pmol/mg*	B_{max} ([#]low) *pmol/mg*
WT	8.62 ± 0.15	6.52 ± 0.19	7.2 ± 1.5	188 ± 3
G243A/I247A	[$]8.14 ± 0.08	6.55 ± 0.22	9.7 ± 1.5	138 ± 36
F240C	9.31 ± 0.04	7.45 ± 0.03	0.4 ± 0.1	29 ± 5
F240C (CuP)	*8.43 ± 0.18	7.25 ± 0.26	2.5 ± 0.8	21 ± 11
G243C	8.85 ± 0.18	6.84 ± 0.04	2.0 ± 0.7	84 ± 11
G243C (CuP)	8.80 ± 0.30	7.13 ± 0.20	2.0 ± 0.9	47 ± 11
A246C	9.46 ± 0.30	7.24 ± 0.14	0.6 ± 0.3	79 ± 10
A246C (CuP)	*8.18 ± 0.23	7.35 ± 0.13	6.1 ± 2.1	58 ± 26
I247C	9.25 ± 0.16	7.14 ± 0.03	1.7 ± 0.9	104 ± 24
I247C (CuP)	8.93 ± 0.40	7.25 ± 0.31	3.2 ± 1.6	*37 ± 1
A250C	8.87 ± 0.10	6.95 ± 0.14	2.7 ± 1.0	79 ± 12
A250C (CuP)	8.83 ± 0.05	7.13 ± 0.06	1.9 ± 0.3	60 ± 10

Molecular Pharmacology Fast Forward. Published on May 8, 2009 as DOI: 10.1124/mol.109.055756
This article has not been copyedited and formatted. The final version may differ from this version.

TABLE 4

Distances between residues from complementary TM IV segments of the intact secretin receptor homo-dimer (Å)

*Note: distances were measured between C_β atoms of the residues, except for glycine for which C_α atoms were used.

Q235-Q235	14.7
G236-G236*	6.2
A239-A239	9.0
F240-F240	4.4
G241-G241*	12.3
W242-W242	14.5
G243-G243*	6.6
S244-S244	12.1
P245-P245	17.0
A246-A246	9.2
I247-I247	6.2
F248-F248	15.6
V249-V249	14.3
A250-A250	3.8

Figure 1

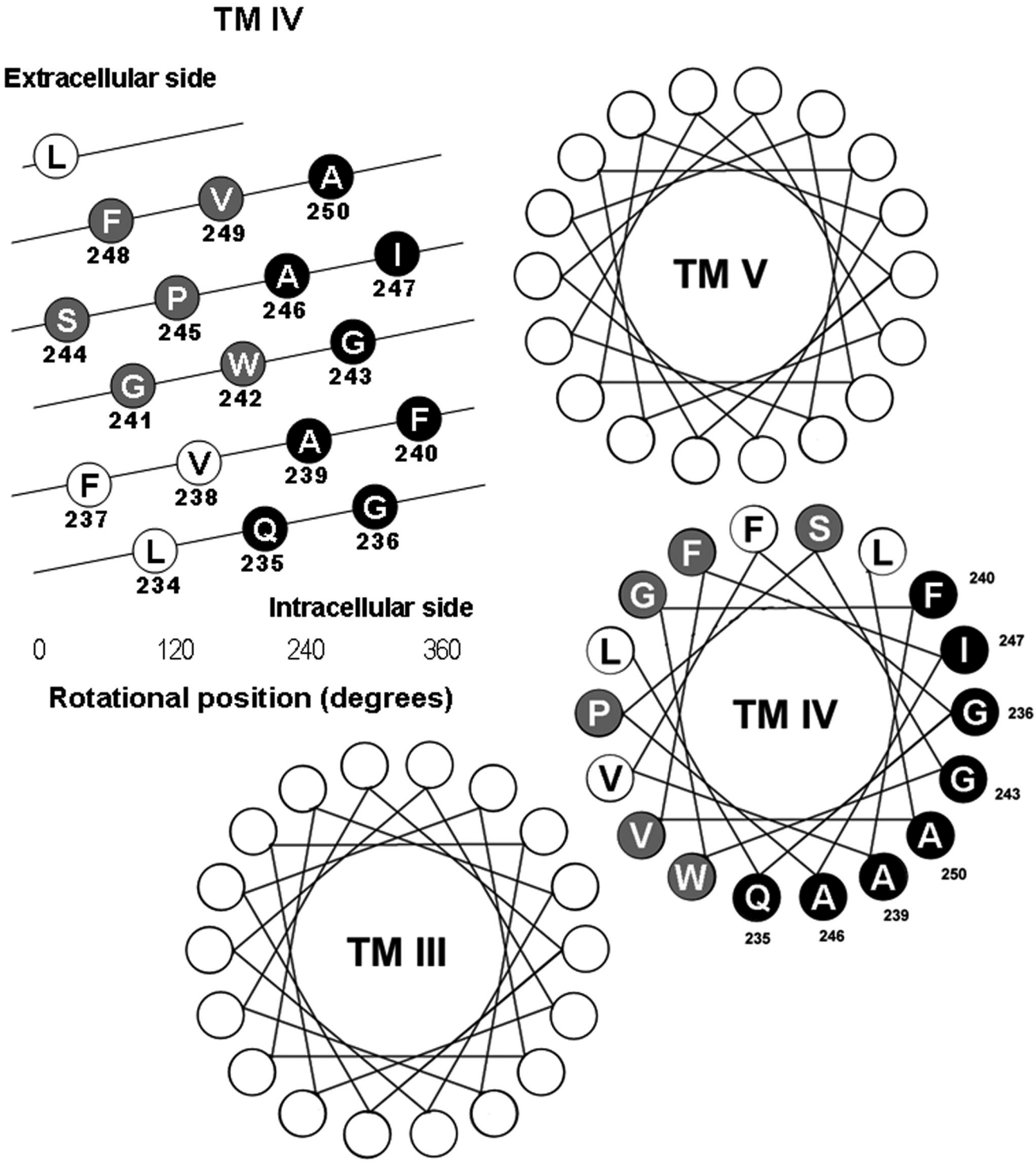
TM IV
Extracellular side
L
F
V
A
248
249
250
S
P
A
I
244
245
246
247
G
W
G
241
242
243
F
V
A
F
237
238
239
240
L
Q
G
234
235
236
Intracellular side
0
120
240
360
Rotational position (degrees)
TM V
TM IV
TM III
F
S
L
F
G
L
P
V
V
W
Q
A
A
240
247
236
243
250
239
246
235

Figure 2

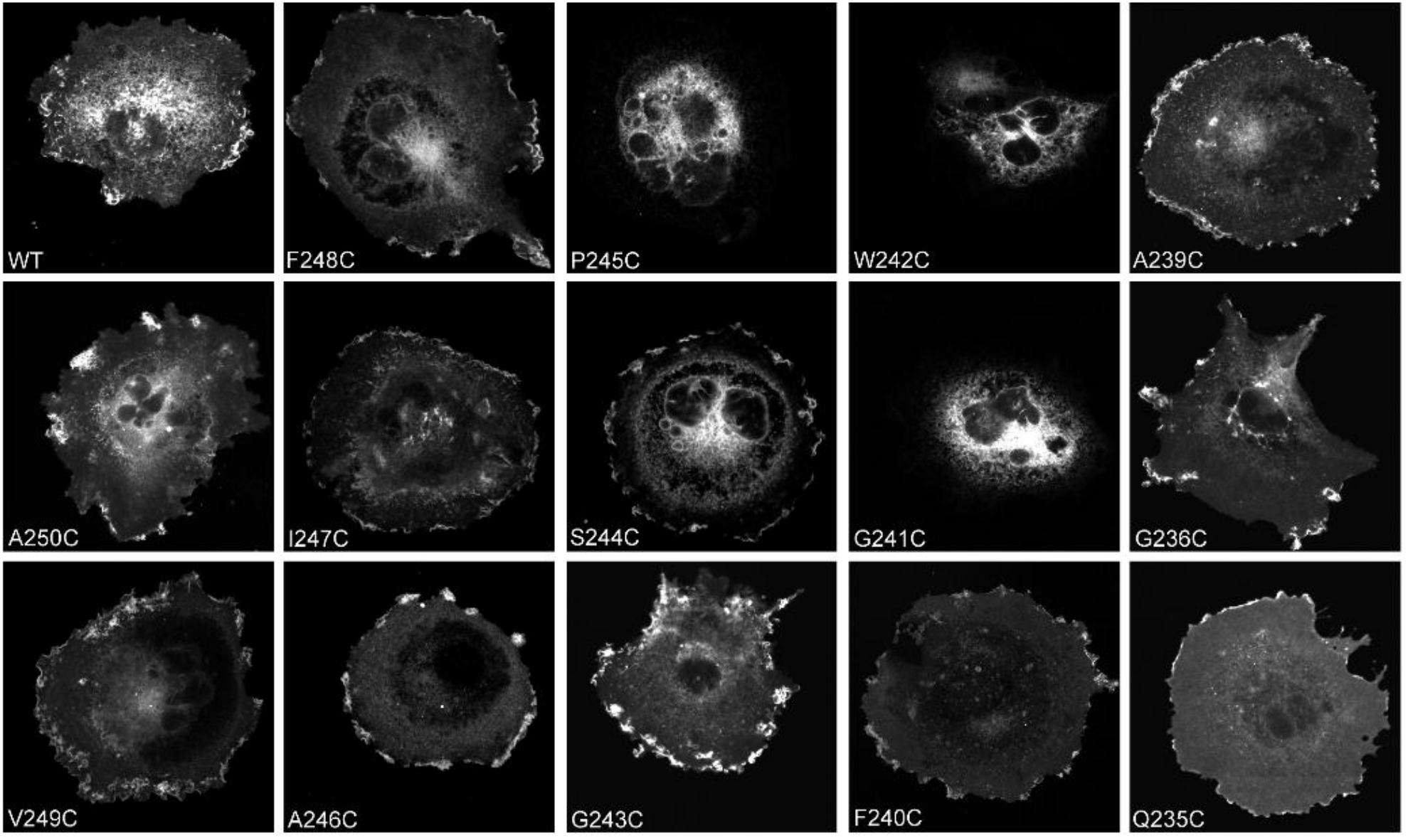
WT
F248C
P245C
W242C
A239C
A250C
I247C
S244C
G241C
G236C
V249C
A246C
G243C
F240C
Q235C

Figure 3

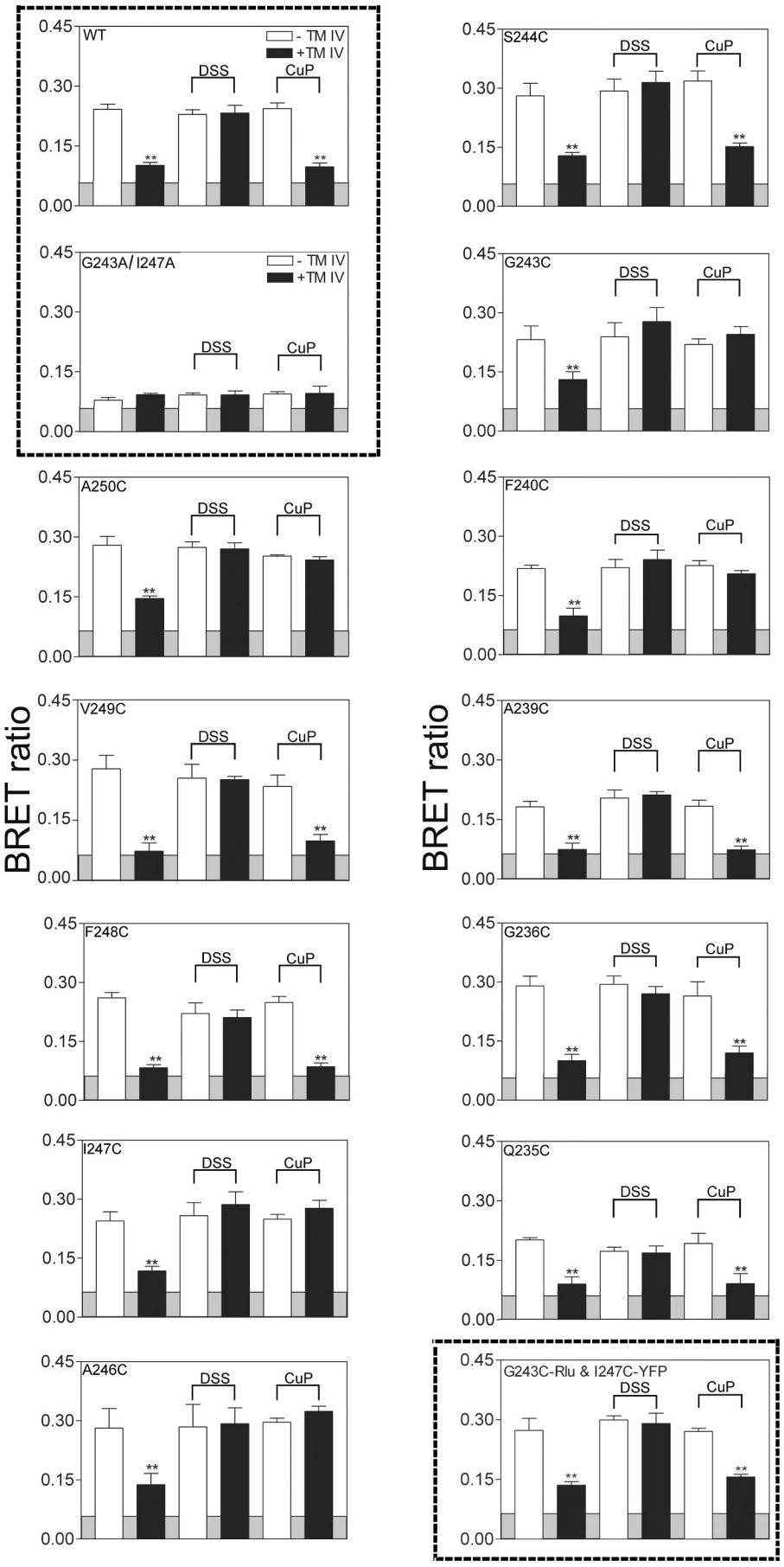
WT
- TM IV
+TM IV
DSS
CuP
G243A/ I247A
S244C
G243C
A250C
F240C
V249C
A239C
F248C
G236C
I247C
Q235C
A246C
G243C-Rlu & I247C-YFP
BRET ratio
0.45
0.30
0.15
0.00
**

Figure 4

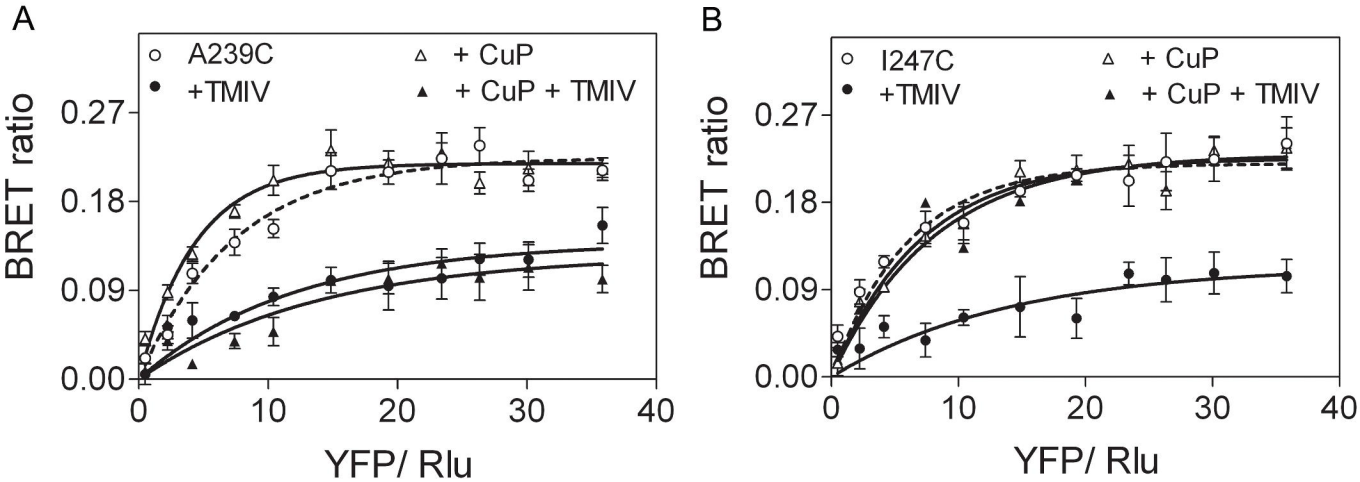
A
A239C
+TMIV
+ CuP
+ CuP + TMIV
BRET ratio
0.27
0.18
0.09
0.00
0
10
20
30
40
YFP/ Rlu
B
I247C
+TMIV
+ CuP
+ CuP + TMIV
BRET ratio
0.27
0.18
0.09
0.00
0
10
20
30
40
YFP/ Rlu

Figure 5

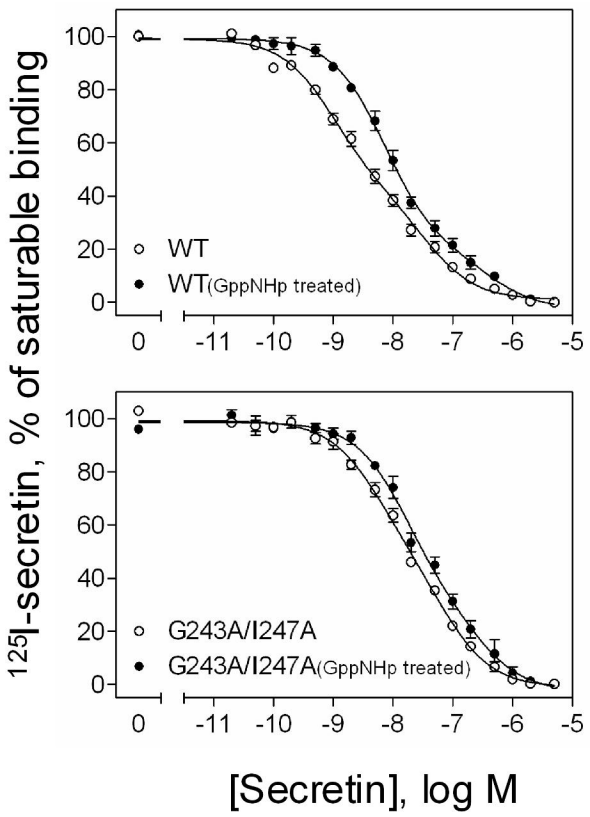
100
80
60
40
20
0
WT
WT(GppNHp treated)
0
-11
-10
-9
-8
-7
-6
-5
100
80
60
40
20
0
G243A/I247A
G243A/I247A(GppNHp treated)
0
-11
-10
-9
-8
-7
-6
-5
125I-secretin, % of saturable binding
[Secretin], log M

Figure 6

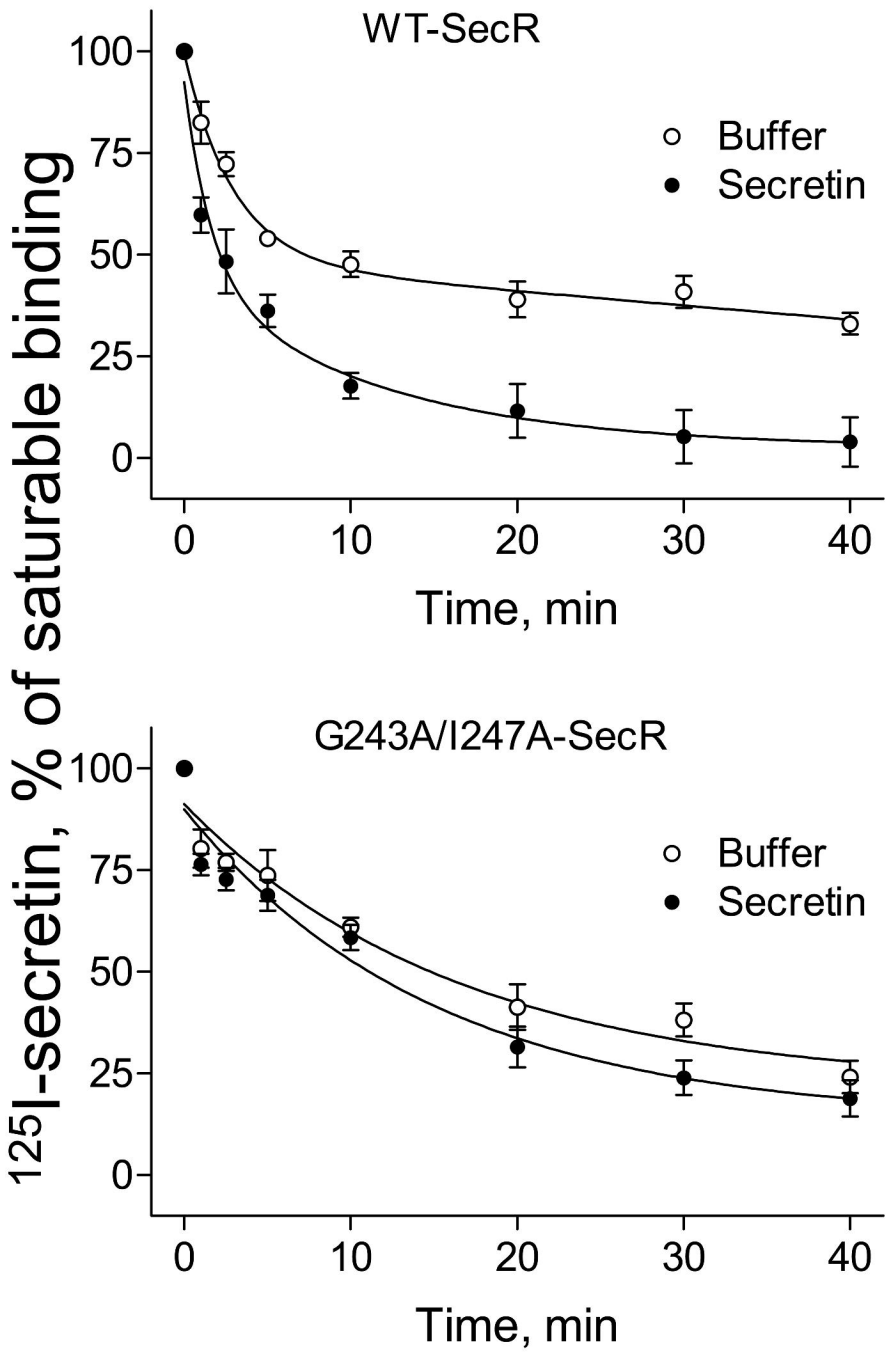
WT-SecR
Buffer
Secretin
100
75
50
25
0
0
10
20
30
40
Time, min
G243A/I247A-SecR
Buffer
Secretin
100
75
50
25
0
0
10
20
30
40
Time, min
125I-secretin, % of saturable binding

Figure 7

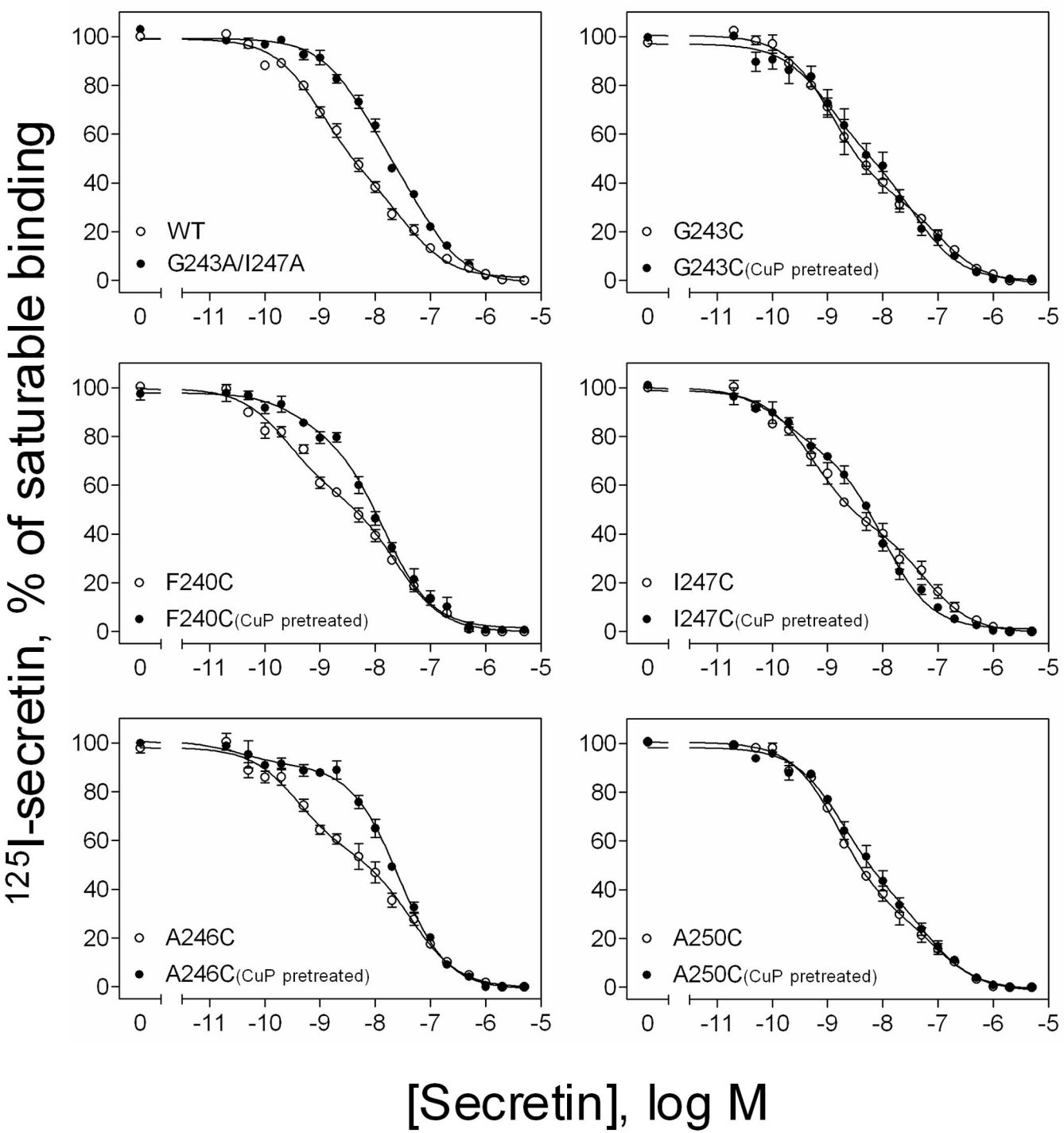
125I-secretin, % of saturable binding
[Secretin], log M
WT
G243A/I247A
G243C
G243C(CuP pretreated)
F240C
F240C(CuP pretreated)
I247C
I247C(CuP pretreated)
A246C
A246C(CuP pretreated)
A250C
A250C(CuP pretreated)

Figure 8

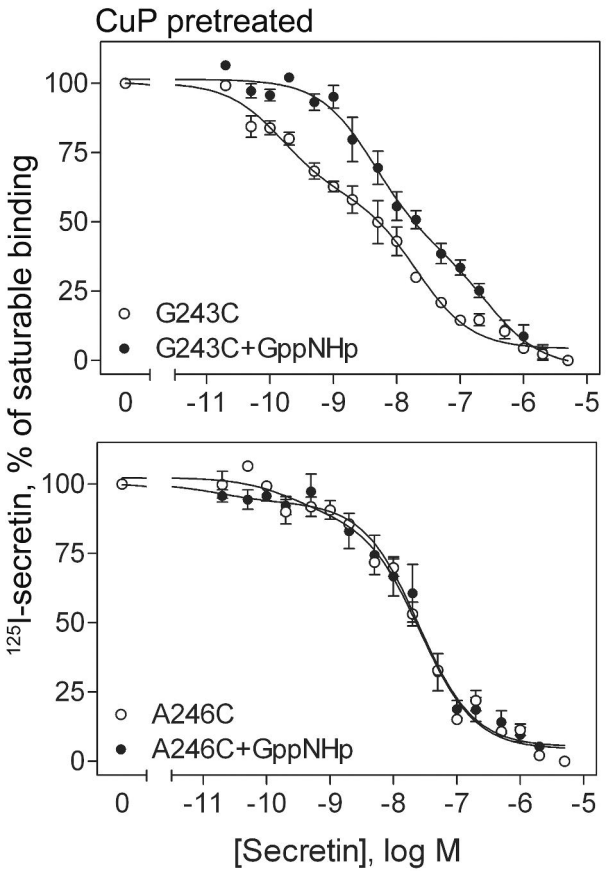
CuP pretreated
100
75
50
25
0
G243C
G243C+GppNHp
0
-11
-10
-9
-8
-7
-6
-5
^{125}I-secretin, % of saturable binding
A246C
A246C+GppNHp
[Secretin], log M

Figure 9